

Optical flashes, reverse shocks and magnetization

Andreja Gomboc^{*}, Shiho Kobayashi[†], Carole G. Mundell[†], Cristiano Guidorzi^{†,**},
Andrea Melandri[†], Iain A. Steele[†], Robert J. Smith[†], David Bersier[†], David Carter[†]
and Michael F. Bode[†]

^{*}*Faculty of Mathematics and Physics, University of Ljubljana, Jadranska 19, SI-1000 Ljubljana, Slovenia*

[†]*Astrophysics Research Institute, Liverpool John Moores University, Twelve Quays House, Egerton Wharf,
Birkenhead, CH41 1LD, UK*

^{**}*INAF-Osservatorio Astronomico di Brera, via Bianchi 46, I-23807 Merate (LC), Italy*

Abstract. Despite the pre-Swift expectation that bright optical flashes from reverse shocks would be prevalent in early-time afterglow emission, rapid response observations show this not to be the case. Although very bright at early times, some GRBs such as GRB 061007 and GRB 060418, lack the short-lived optical flash from the reverse shock within minutes after the GRB. In contrast, other optical afterglows, such as those of GRB 990123, GRB 021211, GRB 060111B, GRB 060117, GRB 061126, and recently GRB 080319B, show a steep-to-flat transition within first 10^3 s typical of a rapidly evolving reverse + forward shock combination. We review the presence and absence of the reverse shock components in optical afterglows and discuss the implications for the standard model and the magnetization of the fireball. We show that the previously predicted optical flashes are likely to occur at lower wavelengths, perhaps as low as radio wavelengths and, by using the case of GRB 061126 we show that the magnetic energy density in the ejecta, expressed as a fraction of the equipartition value, is a key physical parameter.

Keywords: gamma-ray sources; gamma-ray bursts

PACS: 98.70.Rz

THEORY OF OPTICAL FLASHES AND LIGHT CURVE TYPES

The theory of GRB afterglows predicts that when the shell of the relativistically expanding fireball collides with the surrounding medium, a forward shock is formed which, via synchrotron radiation, produces the afterglow emission [1, 2, 3]. In addition, a reverse shock, propagating backwards through the shell, is formed. This reverse shock is predicted, under certain conditions, to produce a bright optical emission - often termed an optical flash [4].

In studying the evolution of relativistic shells and resultant afterglows, one can consider two limiting cases: (i) the thick, low density shell case in which the reverse shock quickly becomes relativistic and begins to decelerate the shell material; and (ii) the thin, high density shell case, in which the reverse shock is too weak to decelerate the shell effectively and the reverse shock does not become relativistic before the shell crossing time (i.e. it remains Newtonian or sub-relativistic). The resulting light curves of the reverse shock in both cases are shown in Figs. 2 and 3 in [5].

When combining the predicted reverse shock emission with the afterglow emission from the forward shock, one obtains three types of light curves [6, 7] (see Fig. 1):

- in Type I, the peak of reverse shock is comparable to or higher than that of the forward shock. The peaks are well separated in time, which makes them both clearly visible.
- in Type II, the peak of the forward shock is weaker and is hidden by the bright reverse shock emission. The forward shock component becomes evident only later, when the reverse shock emission has faded.
- in Type III, the reverse shock emission is fainter and it is hidden by the forward shock emission at all times.

The theory [8, 9] predicts that the strength of the reverse shock emission depends on magnetization (and whether the typical frequency is close to the optical band). The commonly used parameter for magnetization is σ , which is the ratio between the magnetic and kinetic energy flux. For $\sigma \ll 1$, the jet is baryonic and magnetic fields are assumed to be produced via local instabilities at shocks. If the magnetic field originates at the central engine, and advect outwards with the expanding outflow, σ could be large. The reverse-shock peak flux increases with σ initially and starts to decrease when $\sigma \sim 1$. Therefore, in order to obtain bright reverse shock emission, σ should be close to unity.

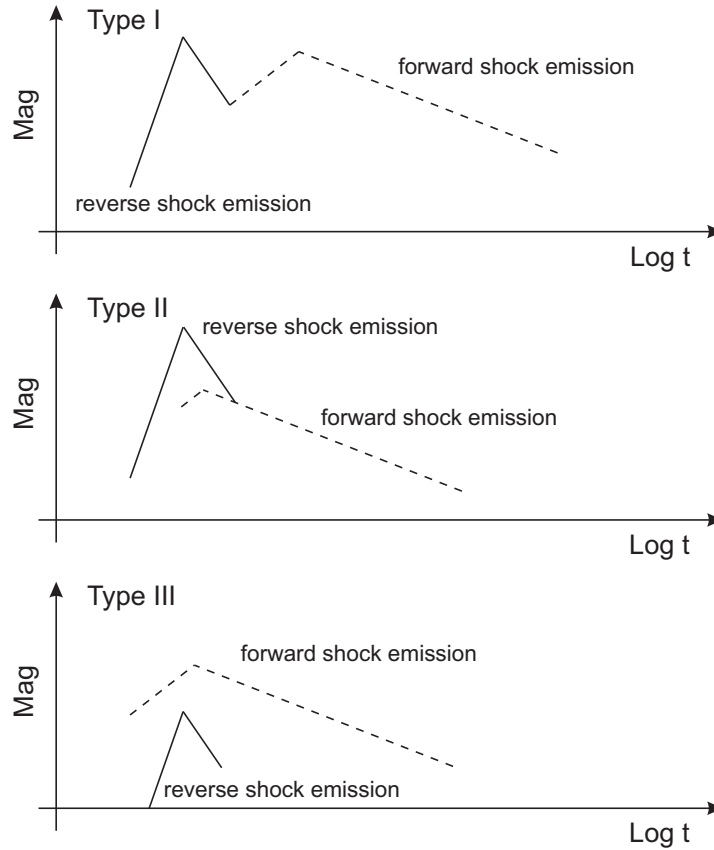


FIGURE 1. Three types of GRB early optical afterglows, produced as a composition of the reverse and forward shock emission [6, 7]. Solid line represents reverse shock emission, and dashed line the forward shock emission.

OBSERVATIONS AND THE LACK OF OPTICAL FLASHES?

Detections in the pre-Swift Era

Before the launch of Swift, there were three optical afterglows detected, which showed the reverse shock emission signature:

- **GRB 990123** was the most famous one: its bright optical flash peaked at 8.9 mag [10] and it was interpreted as due to the reverse shock, decaying with $\alpha \sim 2$ ($F \propto t^{-\alpha}$). From about 10^3 s after the trigger onwards, a more slowly decaying forward shock component with $\alpha \sim 1.1$ became dominant [11, 12, 13]. According to the above classification, this was a burst of Type II.
- **GRB 021004** had an early peak followed by a later re-brightening at about 0.1 days after the trigger. The features in the light curve were modeled with refreshed shocks [14] and the effects of density enhancements in the ambient circumburst medium [15]. The light curve was also consistent with a reverse-shock peak followed by a forward-shock peak [16] and would therefore belong in Type I class.
- **GRB 021211**: no peak was detected in this case, but the optical light curve underwent a flattening from $\alpha \sim 1.6$ to ~ 0.8 at about 11 min after the trigger [17, 18, 19]. It could be interpreted as a Type II reverse plus forward shock afterglow, but with no reverse shock peak caught.

After the detection of the bright optical flash of GRB 990123, expectations of early time observations were high (however, see also [20]). Especially in the Swift era, detections of numerous bright optical flashes were expected, due to rapid and accurate GRB localizations by Swift being fed to large ground-based robotic telescopes capable of immediate follow-up observations.

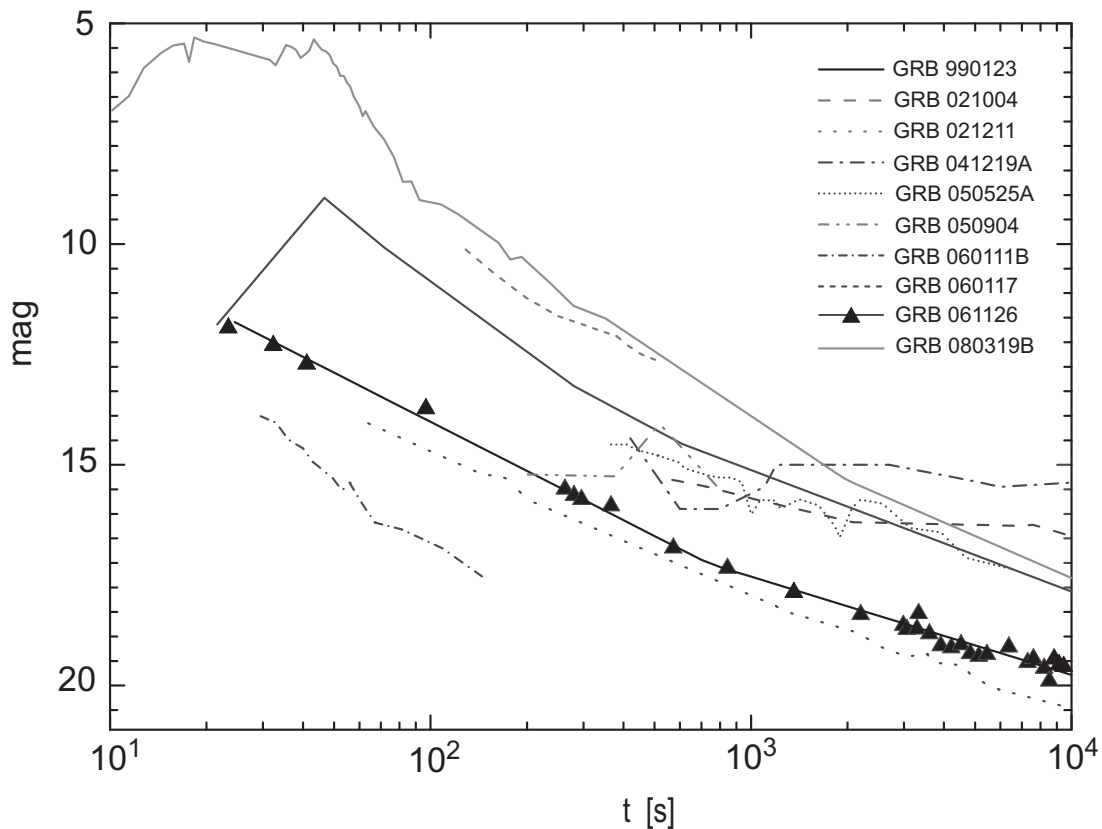


FIGURE 2. Optical afterglow of GRB 061126. Afterglows of GRB 990123, GRB 021004, GRB 021211, GRB 041219A, GRB 050525A, GRB 050904, GRB 060111B, GRB 060117, and GRB 080319B are shown schematically for comparison.

Reverse-Shock Detections in the Swift-Era

Intriguingly, despite high quality ground- and space-based followup observations, there was a dearth of optical flashes. A study of early Swift observations with UVOT offered some interpretations and drove changes in observing strategies [21]. More recently, we analysed a sample of 63 GRBs observed between October 2004 and July 2007 by 2-m robotic Liverpool and Faulkes Telescopes¹ presented in [23]. In this sample, 24 optical afterglows were detected, but only one - GRB 061126 (see below) - optical emission consistent with a reverse shock signature. The remaining 39 GRBs had no detectable optical afterglows despite deep, early time optical observations in red filters. The key question therefore remains- why do bright optical flashes remain elusive?

A full summary of detections of the optical afterglows with a possible reverse shock component in the Swift Era is as follows:

- **GRB 041219A** was studied in [24, 25], who showed that its early optical-IR emission could be understood as a sum of reverse and forward shock emission of Type I.
- **GRB 050525A** could also be classified as of Type I, if its rebrightening at 0.01-0.03 days after the trigger [26] is attributed to the forward shock peak [27, 28].
- **GRB 050904** was at $z=6.3$ [29] one of the most distant GRBs detected. In spite of its distance, it showed a bright optical afterglow, which could be explained with the external forward-reverse shock model or with the "late internal shock model" [30, 31].

¹ For details see [22] and <http://www.astro.livjm.ac.uk/RoboNet/>.

- **GRB 060111B** had an optical light curve of Type II: a fast decaying phase with $\alpha \sim 1.4$ dominated from 28 s to 80 s after the trigger, and was followed by a shallower decay with $\alpha \sim 1.1$ [32].
- **GRB 060117** had a flattening optical light curve, which could be explained as Type II, summing reverse and forward shock emission (with $\alpha_r \sim 2.5$ and $\alpha_f \sim 1.5$) and no reverse shock *peak* detected [33].
- **GRB 061126** also showed a flattening, Type II, optical light curve, which was well covered by observations from 21 s to 15 days after the trigger (see Fig. 2). This case is presented in detail in [34] and [35]. Although observations started very early, they did not catch the rise of the afterglow. The light curve at early time however shows the steeply decaying reverse-shock component to ~ 13 min after the trigger. After this time, the light curve is dominated by the forward shock emission. Analysis presented in [35] shows that the decay indices of the reverse and forward shocks of $\alpha_r = 1.69 \pm 0.09$ and $\alpha_f = 0.78 \pm 0.04$ respectively are in agreement with those expected from the standard model for $p = 2$, which follows from the observed $\beta_X \sim 1$. However, the X-ray afterglow decays faster than the optical (with $\alpha_X \sim 1.3$) and is not in agreement with the standard model. This could indicate a different origin of the X-ray afterglow, which would perhaps also explain two other intriguing properties of this burst: (i) its optical "darkness" at early time: the ratio of optical to X-ray flux places this burst in the "dark burst" region in the Jakobsson plot [36], despite its afterglow being bright, $R \sim 12$ mag, at the beginning of observations, and (ii) a possible chromatic break: a break seen in optical light curve a few days after the trigger that absent from the X-ray light curve, which showed no break.
- **GRB 080319B** was a recent case of an optical flash, the well known naked-eye burst [37]. The observational coverage of its optical emission was unprecedented. It showed Type II characteristics and two steep-to-flat transitions from $\alpha \sim 6.5$ to $\alpha \sim 2.5$ at about 100 s after the trigger, to $\alpha \sim 1.25$ at about 10^3 s after the trigger. As this is a well-studied burst, we refer the reader to e.g. [37] for more detail.

GRBs lacking Reverse Shock Emission in the Swift-Era

In addition to GRBs with bright afterglows consistent with reverse shock emission at early time, GRBs with bright optical counterparts have also been detected that are not consistent with reverse shock emission.

One explanation for the absence of bright reverse-shock emission is suppression due to a high degree of magnetization of the fireball. In the case of GRB 060418, which showed Type III optical afterglow, there is another option to explain the absence of a distinctive reverse shock component. Even in the standard model, if the typical frequency of the forward shock is already below the optical band at the shock crossing time, the two shock emissions peak at the same time, and they contribute equally to the observed optical light. The superposition produces a single peak. Using the RINGO polarimeter [38] mounted on the Liverpool Telescope, an automatic measurement of the early-time polarization of the GRB 060418 afterglow was taken at its peak, i.e. at the onset of the afterglow [39]. A low upper limit of 8% shows that no large-scale ordered magnetic field is actually needed or that very strong magnetic field $\sigma \gg 1$ suppresses the reverse shock emission.

A low typical frequency of the reverse shock, which is lower by a factor of Γ^2 than that of forward shock, also explains the lack of optical flash in GRB 061007 [40]. The bright optical afterglow ($R > 10.3$ mag) was observed from 137 s to 10^5 s after the trigger and showed only a simple decay with $\alpha \sim 1.7$. This afterglow was explained with forward shock emission, while the typical frequency of the reverse shock emission lies in radio wavebands already at the beginning of observations at 137 s after the trigger.

Other possible explanations for the paucity of optical flashes that have been suggested are: dust extinction [41, 42, 43, 44], and the inverse Compton process, in which most of the energy is emitted through IC process and synchrotron component is suppressed [45]. Most commonly, though, strong suppression of the reverse shock in the Poynting-flux dominated outflow is considered [8, 9, 46]. Some new theoretical results seem to indicate that even a mild magnetization can suppress a reverse shock [47, 48, 49].

OBSERVATIONS AND MAGNETIZATION

We may use those GRBs with reverse shock signature to study the magnetization of the fireball. We define parameter $R_B = \epsilon_{B,r}/\epsilon_{B,f}$ as the ratio of magnetic equipartition parameters in the reverse shock and forward shock (Note that the definition of the magnetization is different from that in [6]). Results for some of the above mentioned GRBs are the following:

- GRB 990123: $R_B \sim 200$ [6],
- GRB 021004: $R_B \sim 1$ [6],
- GRB 021211: $R_B \geq 1$ [6, 50],
- GRB 041219A: $R_B \sim 10$ [25],
- GRB 061126: $R_B \sim 50$ [35].

These results imply that magnetic energy density in the reverse shock is equal to or larger than that in the forward shock. Nevertheless, since $\epsilon_{B,f} \sim 10^{-4} - 10^{-2}$ is usually inferred from afterglow modeling [51], it follows that $\epsilon_{B,r} < 1$. Therefore, in all the above cases we are dealing with mildly magnetized outflow and not a Poynting flux dominated outflow.

Polarization

Theoretical models predict that mildly magnetized outflows produce strong reverse shock emission and that this emission should be polarized [52, 53, 54, 9, 55]. Therefore, polarization measurements at very early times are of key importance to distinguish between the usual baryon-rich fireball model and the Poynting flux-dominated outflow model.

The predicted very early afterglow (possibly even an optical flash) should be strong enough not only to be detected by current robotic telescopes, but also to make polarimetry measurements possible. This was the motivation behind the RINGO polarimeter on the Liverpool Telescope: the Liverpool Telescope is able to commence observations in ~ 100 s after the trigger and is capable of good polarimetric accuracy for bright targets (for details see [38]). The feasibility of such early polarimetry was demonstrated in the case of GRB 060418 [39]. This burst was of Type III, with hidden reverse shock component. It would be of even greater interest to measure the early polarization of an afterglow with the prominent reverse shock contribution or even during the reverse shock peak (Type I or II). This would provide further additional constraints on the presence of magnetized fireballs.

CONCLUSIONS

The absence of a large number of optical flashes might be explained with the standard reverse shock model via weak, non-relativistic reverse shocks and a typical frequency well below the optical band [5]. Some optical flashes may be suppressed by a strong magnetic field, although new theoretical results suggest that even mild magnetization may suppress a reverse shock. Catching more GRBs with reverse shock components is important for distinguishing between these possibilities, understanding reverse shocks and the role of magnetization. Magnetization is a fundamental and yet unsolved issue of GRB physics. Early polarimetry may be of the key importance to help solve this issue, since it may prove to be a truly needed independent probe of the physical conditions of the GRB afterglow.

ACKNOWLEDGMENTS

AG thanks Slovenian Research Agency and Slovenian Ministry for Higher Education, Science, and Technology for financial support. C.G. acknowledges support from ASI grant I/011/07/0. CGM acknowledges financial support from the Royal Society and Research Councils U. K. *RoboNet-1.0* was supported by PPARC and STFC. *Swift* mission is funded in the UK by STFC, in Italy by ASI, and in the USA by NASA. The Faulkes Telescopes are operated by the Las Cumbres Observatory. The Liverpool Telescope is owned and operated by Liverpool John Moores University.

REFERENCES

1. R. Sari, and T. Piran, *ApJ*, **455**, L143-L146 (1995).
2. P. Mészáros, and M. J. Rees, *ApJ*, **476**, 232-237 (1997).
3. R. Sari, T. Piran, and R. Narayan, *ApJ*, **497**, L17-L20 (1998).
4. R. Sari, and T. Piran, *ApJ*, **520**, 641-649 (1999).
5. S. Kobayashi, *ApJ*, **545**, 807-812 (2000).
6. B. Zhang, S. Kobayashi, and P. Mészáros, *ApJ*, **595**, 950-954 (2003).
7. Z. P. Jin, and Y. Z. Fan, *MNRAS*, **378**, 1043-1048 (2007).
8. B. Zhang, and S. Kobayashi, *ApJ*, **628**, 315-334 (2005).
9. Y. Z. Fan, D. M. Wei, and C. F. Wang, *A&A*, **424**, 477-484 (2004).
10. C. Akerlof et al., *Nature*, **398**, 400-402 (1999).
11. R. Sari, and T. Piran, *ApJ*, **517**, L109-L112 (1999).
12. P. Mészáros, and M. J. Rees, *MNRAS*, **306**, L39-L43 (1999).
13. E. Nakar, and T. Piran, *ApJ*, **619**, L147-L150 (2005).
14. B. Zhang and P. Mészáros, *ApJ*, **566**, 712-722 (2002).
15. D. Lazzati et al., *A&A*, **396**, L5-L9 (2002).
16. S. Kobayashi, and B. Zhang, *ApJ*, **582**, L75-L78 (2003).
17. D. W. Fox et al., *ApJ*, **586**, L5-L8 (2003).
18. S. B. Pandey et al., *A&A*, **408**, L21-L24 (2003).
19. D. M. Wei, *A&A*, **402**, L9-L12 (2003).
20. C. Akerlof et al. *ApJ*, **532**, L25-L28 (2000).
21. P. W. A. Roming et al., *ApJ*, **652**, 1416-1422 (2006).
22. A. Gomboc et al, *Nouvo Cimento C*, **10**, 1303-1306 (2006).
23. A. Melandri et al., *ApJ*, **686**, 1209-1230 (2008).
24. C. H. Blake et al., *Nature*, **435**, 181-184 (2005).
25. Y. Z. Fan, B. Zhang, and D. M. Wei, *ApJ*, **628**, L25-L28 (2005).
26. A. Klotz et al., *A&A*, **439**, L35-L38 (2005).
27. L. Shao, and Z. G. Dai, *ApJ*, **633**, 1027-1030 (2005).
28. A. J. Blustin et al., *ApJ*, **637**, 901-913 (2006).
29. G. Tagliaferri et al., *A&A*, **443**, L1-L5 (2005).
30. D. M. Wei, T. Yan, and Y. Z. Fan, *ApJ*, **636**, L69-L72, (2006).
31. M. Boër et al., *ApJ*, **638**, L71-L74, (2006).
32. A. Klotz et al., *A&A*, **451**, L39-L42 (2006).
33. M. Jelinek et al., *A&A*, **454**, L119-L122 (2006).
34. D. A. Perley et al., *ApJ*, **672**, 449-464 (2008).
35. A. Gomboc et al., *ApJ*, **687**, 443-455 (2008).
36. P. Jakobsson et al., *ApJ*, **617**, L21-L24 (2004).
37. J. L. Racusin et al. *Nature*, **455**, 183-188 (2008).
38. I. A. Steele et al., in *Ground-based and Airborne Instrumentation for Astronomy*, Edited by McLean, Ian S.; Iye, Masanori. Proceedings of the SPIE, Volume 6269, pp. 62695M (2006).
39. C. G. Mundell et al., *Science*, **315**, 1822-1824 (2007).
40. C. G. Mundell et al., *ApJ*, **660**, 489-495 (2007).
41. A. M. Soderberg, and E. Ramirez-Ruiz, *330*, L24-L28 (2002).
42. R. L. C. Starling et al., *ApJ*, **661**, 787-800 (2007).
43. P. Schady et al., *MNRAS*, **377**, 273-284 (2007).
44. A. Li et al., *ApJ*, **685**, 1046-1051 (2008).
45. S. Kobayashi et al., *ApJ*, **655**, 391-395 (2007).
46. Y. Mizuno et al., arXiv:0810.2779v1 (2008).
47. P. Mimica, D. Giannios, and M. A. Aloy, arXiv:0810.2961v1 (2008).
48. Y. Z. Fan, arXiv:0808.0511v1 (2008).
49. D. Giannios, P. Mimica, and M. A. Aloy, *A&A*, **478**, 747-753 (2008).
50. P. Kumar and A. Panaitescu, *MNRAS*, **346**, 905-914 (2003).
51. A. Panaitescu, and P. Kumar, *ApJ*, **571**, 779-789 (2002).
52. M. Lyutikov, V. I. Pariev, and R. D. Blandford, *ApJ*, **597**, 998-1009 (2003).
53. J. Granot and A. Königl, *ApJ*, **594**, L83-L87 (2003).
54. E. M. Rossi et al., *MNRAS*, **354**, 86-100 (2004).
55. S. Covino, *Science*, **315**, 1798-1799 (2007).